MACHOS IN THE SOLAR NEIGHBOURHOOD

B. FUCHS, H. JAHREISS
Astronomisches Rechen–Institut Heidelberg,
Mönchhofstr. 12–14, 69120 Heidelberg, Germany

We rediscuss the question of what fraction of the population of MACHOs in the halo of the Milky Way might be in the form of halo dwarfs, because recent determinations indicate masses of the MACHOs, which are typical for such stars. For this purpose we have analyzed the Third Catalogue of Nearby Stars and identified the subdwarfs and a high velocity white dwarf in the solar neighbourhood. The local mass density of these stars is $1.5{\cdot}10^{-4}$ $\mathcal{M}_\odot$ pc^{-3}, which is only 3% of the current estimate of the local mass density of the MACHO population. We compare the local density of subdwarfs with constraints set by HST observations of distant red dwarfs. Using models of the stellar halo with density laws that fall off like $r^{-\alpha}$, $\alpha = 3.5$ to 4, we find that the HST constraints can only be matched, if we assume that the stellar halo is flattened with an axial ratio of about 0.6. The non–detection of the analogs of MACHOs in the solar neighbourhood allows to set an upper limit to the luminosity of MACHOs of $M_B > 21$ magnitudes.

1 Introduction

The MACHO [1] and EROS [2] collaborations have reported new results of their campaigns of observing micro-lensing events towards the LMC. These indicate that MACHOS have masses typically of half a solar mass and contribute about one half to the mass budget of the halo of the Milky Way (see the article by Bennett in this volume). Such masses are typical for red and white dwarfs. Bahcall and collaborators [3,4] have made by very deep star counts based on HST data *in situ* measurements of the space density of such stars in regions, where the micro-lenses are expected to be physically located. Their conclusion is that halo dwarfs contribute only a few percent to the mass of the halo and are thus unlikely MACHO candidates. Graff & Freese [5] (see also Freese's article in this volume) infer from the same data that the local mass density of halo dwarfs is even less than one percent of the combined local densities of the dark and stellar halos.

On the other hand, halo dwarfs are directly observed in the solar neighbourhood. Liebert [6] discusses the results of the USNO parallax programme for red dwarfs and finds that the number of halo dwarfs in that sample is consistent with the HST data. We have followed a complementary approach. Recently the Third Catalog of Nearby Stars (CNS3) [7] has been completed at the Astronomisches Rechen-Institut. This provides the now most complete inventory of the solar neighbourhood up to a distance of 25 pc from the Sun

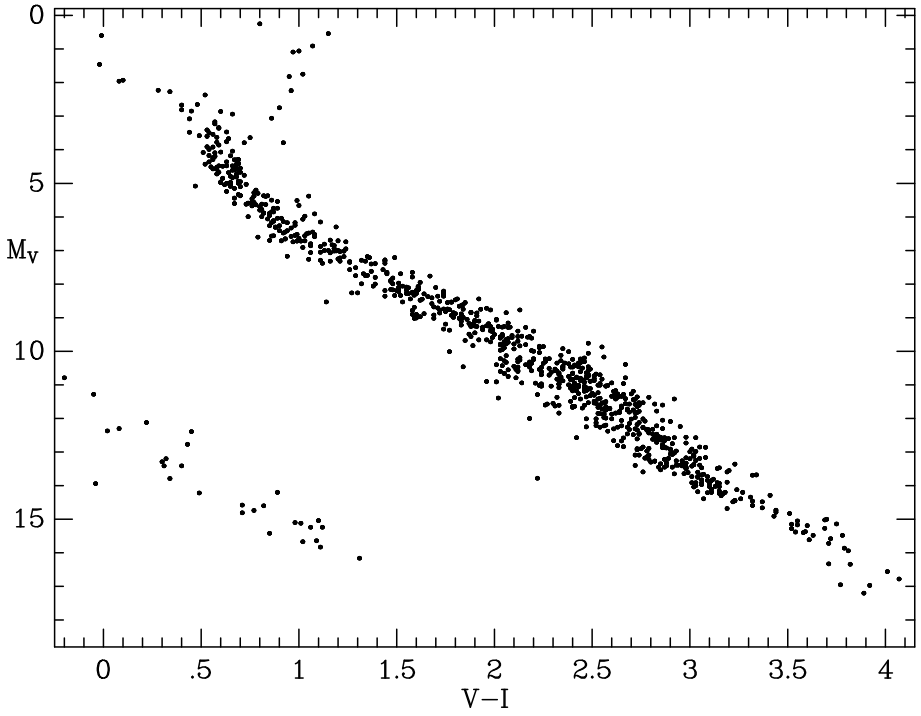

Figure 1: Colour–Magnitude diagram of nearby stars with $\sigma_{M_V} \leq 0.3$ mag.

and allows a new determination of the local density of halo stars.

2 Subdwarfs in the CNS3

We have searched the CNS3 for halo dwarfs. These reveal themselves by their position on the subdwarf sequence in the colour-magnitude diagram (CMD), their low metallicity, and their high space velocities. Unfortunately, there is in this metallicity range a broad overlap of the comparatively few halo stars and the much more abundant thick disk stars. We have therefore adopted a very conservative search strategy in order to isolate a true halo population, even if this will lead to an undersampling of the halo population. We have examined first the stars on the subdwarf sequence, which can be clearly seen in the CMD shown in Fig. 1. The reliability of the photometry and the parallaxes of each star has been checked carefully, which led to the omission of quite a number

Table 1: Subdwarfs in the CNS3.

	d	M_V	$V-I_c$	U	V	W	[Fe/H]	$\mathcal{M}$
	[pc]	[mag]	[mag]		[km/s]			$[\mathcal{M}_\odot]$
Gl 191	3.9	10.90	1.98	19	–288	–54	< -1	0.2
Gl 299	6.8	13.65	2.83	107	–126	–45	< -1	0.1
Gl 53A	7.5	5.80	0.79	–42	–157	–34	–0.6	0.73
Gl 53B	7.5	11.00						0.1
Gl 451A	8.9	6.70	0.85	273	–154	–16	< -1	0.6
Gl 699.1	15.6	13.34	0.50	–149	–294	–42		0.6
GJ 1062	16.0	12.00	2.76	93	–212	17	< -1	0.15
Gl 781	16.5	10.91	2.56	104	–47	34	< -1	0.2
Gl 158	18.4	7.17	0.93	–41	–188	21	< -1	0.6
LHS 3409	20.3	13.59	2.76	–31	–101	44	low	0.1
GJ 1064A	23.6	6.31	0.86	–94	–109	–74	–1	0.67
GJ 1064B	23.6	6.91	1.02	–94	–111	–77	< -1	0.63
WO 9722	23.9	11.39	2.05	264	–215	–92	low	0.17
LHS 375	23.9	13.78	2.27		$v_t = 158$		<-1	0.1

of stars with inaccurate parallaxes. In this way we identified Gl 191, Gl 781, WO 9722 = LHS 64, GJ 1062, LHS 375, and LHS 3409 as likely halo stars. A number of stars in the CNS3 are classified as subdwarfs by their spectral type. This enables us to search for subdwarfs in that part of the CMD, $V - I < 1.5$, where the subdwarf sequence comes very close to the main sequence. We include GJ 1064A+B and Gl 53A+B, which have reliable parallaxes, into our list on the basis of this criterion. All stars have decidedly large space velocities (cf. Table 1 and Fig. 2). In addition to these stars we found 4 stars, Gl 158, Gl 299, Gl 451A, and the white dwarf Gl 699.1 (spectral type DA7), which do not lie very prominently on the subdwarf sequence, but have space velocities, which clearly identify them as halo stars.

All the stars in our list have very low metallicities. Leggett [8] has determined the metallicities of a large number of nearby M dwarfs from their position in the (J–H)–(H–K) two infrared-colour diagram. According to that determination Gl 191, Gl 781, GJ 1062, and Gl 299 have metallicities [Fe/H] < -1.

LHS 375 has been classified as a cold subdwarf by Ruiz and Anguita [9]. The metallicities of Gl 53A, Gl 158, Gl 451, and GJ1064A, B have been taken from the compilation by Taylor [10]. Reid et al. [11] have classified GJ 1062, Gl 781 [a], WO 9722, and LHS 3409 as likely subdwarfs on the basis of their spectra. Jones et al. [12] confirm the low metallicity of Gl 299. There are many apparently low metallicity stars in the catalogue, which must be thick disk stars. For instance Leggett [8] has assigned to 20 stars in the CNS3 a metallicity of [Fe/H] < -1, of which only 4 have been finally included in our sample.

In Table 1 we give the list of stars selected out of the CNS3 as described above, of which we are now reasonably certain that they are genuine halo stars. The velocity components of the subdwarfs given in columns 6 to 8 in Table 1 are referred to the Sun. In order to reduce them to the LSR the solar motion (U, V, W)$_\odot$ = (+9, +12, +7) km/s has to be added. Note that U points towards the galactic center. The velocity distribution of our sample is shown as a Toomre diagram in Fig. 2. It is consistent with a distribution centered on V = –220 km/s. No clustering near V = –40 km/s, which would indicate a contamination by thick disk stars, is detected. The dispersion of $\sqrt{U^2 + W^2}$ is 150 ± 30 km/s, which is within statistical errors consistent with other determinations [13] of the kinematical parameters of halo stars. The masses given in the last column of

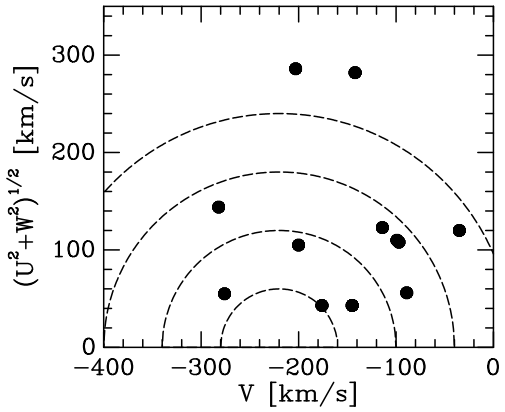

Figure 2: Toomre diagram of the nearby halo dwarfs. The dashed lines indicate lines of constant kinetic energy of the halo stars.

Table 1 have been assigned using the mass-to-luminosity relation calculated theoretically for a metallicity of [Fe/H] = –1.35 by Alexander et al [14].

[a] Gl 781 is a variable star and shows H$_\alpha$ emission. However, it is a spectroscopic binary, which, in our view, accounts for this phenomenon.

3 Results and Discussion

3.1 Local density

The local mass density of halo stars can be estimated in various ways. In Fig. 3 we show density estimates, which have been calculated from the cumulative distribution of the stars in our sample, i.e. by adding up the masses of stars within given distances and dividing by the corresponding spherical volumes. The stars within 10 pc give rather high density estimates of the order of 10^{-3} $\mathcal{M}_\odot$ pc^{-3}. Even though Wielen & Jahreiß [15] found similar values, when evaluating the second edition of the Gliese catalogue, they seem unrealistic to us. We find a plateau in the density run, when we consider the stars within the 20 pc sphere (cf. Fig. 3). Beyond that the density drops off, probably because the catalogue becomes incomplete. The most likely value of the local mass density lies according to this determination in the range 1.5 to $1{\cdot}10^{-4}$ $\mathcal{M}_\odot$ pc^{-3}. The local density of the dark halo [16] is about $9{\cdot}10^{-3}$ $\mathcal{M}_\odot$ pc^{-3} (see also Gates' article in this volume), so that the local density of halo stars is about 1.7% of the halo density or 3% of the local MACHO density as determined by the MACHO collaboration. We have broken down our sample of subdwarfs with

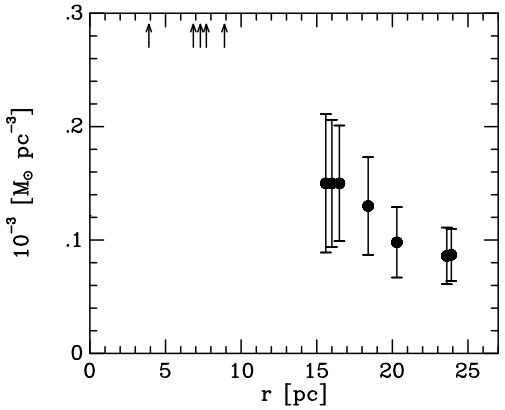

Figure 3: Mass density of nearby halo dwarfs as function of the distance from the Sun. Within 10 pc only the positions of the stars are indicated. The errorbars indicate the statistical uncerntainties.

respect to absolute magnitudes. The resulting 'luminosity function' has been compared with the subdwarf luminosity function obtained by Dahn et al. [17] for stars with $M_V > 10$ mag. Both luminosity functions agree well within statistical errors.

3.2 Matching the constraints by HST data.

It is interesting to confront the density of halo stars derived here with density estimates based on the HST data. Graff & Freese [5] find in a detailed analysis of earlier HST data [3] a value about five times less than our estimate, which is partly due to their restriction to red dwarfs redder than $V - I \approx 2$ mag. Whereas these authors tried to infer the local density of halo stars from the star counts, we reverse the approach and make predictions of the expected number of stars in the star count field. Very recently Flynn et al. [4] have reported an analysis of the Hubble Deep Field (HDF). The HDF has a size of 4.4 square arcminutes and is located at $l = 126°$, $b = 55°$. The limiting magnitudes are 18 to 26.3 mag in the I–band.

In the following we assume that the population of halo stars follows a density law of the form

$$\nu_h = \nu_{h_\odot} \left(\frac{r_c^2 + r_\odot^2}{r_c^2 + r^2} \right)^\alpha \tag{1}$$

with an arbitrarily chosen core radius of $r_c = 1$ kpc. Such density laws are typical for other tracers of the halo population, such as RR Lyr stars [18] or horizontal branch stars [19], in the Milky Way or external galaxies [20]. The exponent α lies typically in the range 3.5 to 4. Note that the dark halo is usually described by a density law of the form as in equation (1) with $\alpha = 2$. If the subdwarfs are observed locally at a density $\nu_{h_\odot}$, one predicts by integrating along the line of sight

$$N = \Omega \nu_{h_\odot} \int_{d_{min}}^{d_{max}} s^2 \left(\frac{r_c^2 + r_\odot^2}{r_c^2 + r_\odot^2 + s^2 - 2 s r_\odot \cos l \cos b} \right)^\alpha ds \tag{2}$$

stars in the star count field. Ω is the angular area of the field and the minimum and maximum distances are determined by the limiting magnitudes. We concentrate first on the colour range $V - I = 1.8$ to 3.5 mag. We have 4 stars in that range within 16.5 pc, where we believe our sample to be reasonably complete. If we project these into the cone towards the HDF, we obtain the star numbers summarized in Table 2. The limiting distances have been calculated for each star individually,

$$d_{\rm min,max} = 10^{0.2(I_{\rm min,max} + (V-I) - M_V + 5)}, \tag{3}$$

where, in order to avoid confusion with disk stars in the HDF, we adopt a lower limit of $I_{min} = 24.6$ mag. As can be seen from Table 2 we predict 7 to 11 stars in the HDF, whereas Flynn et al. [4] have actually dectected no star. Despite

Table 2: Predicted Number of Stars in the HDF and the GS.

		$V-I>1.8$	$V-I<1.8$	
α	c/a	n_{HDF}	n_{HDF}	n_{GS}
3.5	1	11	17	265
4	1	7	7	144
3.5	0.6	4	5	69
4	0.6	2	2	32

the low number of stars involved, this discrepancy seems to be statistically significant. Several explanations might account for this discrepancy. First, the stellar halo might be much more irregular and lumpy than previously thought. Second, the stellar halo is almost certainly flattened [18,19,20] with an axial ratio around c/a ≈ 0.6. If we take such a flattening into account in the halo model,

$$\nu_h = \nu_{h\odot} \left(\frac{r_c^2 + R_\odot^2}{r_c^2 + R^2 + z^2/(c/a)^2} \right)^\alpha \quad , \tag{4}$$

where R, z denote cylindric coordinates, we predict star numbers in the HDF, which are statistically consistent with no star seen by Flynn et al [4].

The star counts in the HDF in the colour range $V-I<1.8$ mag can be interpreted in a similar way. Disk stars in this colour range are so bright that they would have to lie several kpc above the midplane to appear fainter than $I=22$ mag. Thus in order to avoid confusion with disk stars in the HDF, we consider only stars fainter than $I=22$ mag. In our sample there are 4 stars within 20 pc in this colour range. Their $V-I$ colours cluster around 0.9 and the white dwarf has $V-I=0.5$. Thus we define a colour range $0.5<V-I<1.8$, in which we compare the predictions with actually observed numbers of stars. If the stars of our sample are projected into the cone towards the HDF using spherical halo models, we predict 7 to 17 stars depending on the model, whereas Flynn at al. [4] have observed 4 stars. If we assume again a flattening of c/a $= 0.6$, the number of expected stars is consistent with the observed number.

Gould et al. [21] are presently investigating another field observed by HST. This is the so called Groth strip (GS), which has an angular size of 114 square arcminutes and is located at $l=96^\circ$ and $b=60^\circ$. Its limiting magnitude is $I=23.9$ mag. Gould et al. [21] have very kindly made their preliminary data available to us, so that we were able to make star counts in this field. Due to

the limiting magnitude of $I = 23.9$ mag even the faintest stars in the GS with colours redder than $V - I = 1.8$ could be disk stars. Thus we focus on the colour range $V - I < 1.8$ and adopt the same halo zone as in the HDF. The GS has 66 stars in this zone. If we project the local subdwarfs into the cone towards the GS, we obtain the numbers of predicted stars summarized in the last column of Table 2. Again a flattened halo model is a better fit to the data.

3.3 Constraints on the absolute magnitude of MACHOs.

Like previous authors we have *not* detected the analogs to MACHOs in the solar neighbourhood. This raises the question why. All subdwarfs in our sample appear in the LHS high-proper motion star catalogue. Being halo objects, MACHOs in the solar neighbourhood must have similar proper motions. The fact that they have not been found in high-proper motion surveys allows to set an upper limit to their luminosity. The LHS catalogue [22], for instance, is claimed to be complete for stars down to apparent magnitude $B = 21$ mag and with proper motions $2.''5/\mathrm{a} > \mu > 0.''5/\mathrm{a}$. For stars brighter than $B = 10$ mag it is claimed that all stars with proper motions $\mu > 0.''3/\mathrm{a}$ are contained in the catalogue. We assume that the MACHOs are homogeneously distributed around the Sun and have a gaussian velocity distribution,

$$dn = \frac{\nu_{M_\odot}}{(2\pi)^{3/2}\sigma_M^3} exp - \frac{1}{2\sigma_M^2}(U^2 + (V - \overline{V})^2 + W^2) d^3v d^3r \ , \qquad (5)$$

centered on $\overline{V} = -220$ km/s and with a velocity dispersion typical for halo objects, $\sigma_M = \overline{V}/\sqrt{2}$. Integrating now over all radial velocities and the proper motions according to the specifications of the LHS we can determine the radius r_2 of the sphere out of which one would expect say 2 MACHOs in the LHS,

$$\begin{aligned} 2 \ = \ & 4.74^2 \frac{\nu_{M_\odot}}{\sigma_M} \int_0^{r_2} dr r^4 \int_{\mu_l}^{\mu_h} d\mu \mu \int_0^{2\pi} dl \int_{-\pi}^{+\pi} db \cos b \\ & \cdot I_0 \left(\frac{\overline{V}}{\sigma_M^2} 4.74 \mu r \sqrt{1 - \sin^2 l \cos^2 b} \right) \\ & \cdot exp - \frac{1}{2\sigma_M^2} \left(\overline{V}^2 (1 - \sin^2 l \cos^2 b) + (4.74 \mu r)^2 \right) \ , \end{aligned} \qquad (6)$$

where I_0 denotes the Bessel function. According to Poisson statistics two expected MACHOs would be still consistent with no MACHO actually seen in the LHS survey. In Table 3, we give results of numerical integrations of equation (6) assuming a local density of MACHOs of $\nu_{M_\odot} = 0.5 \cdot 0.01 \ \mathcal{M}_\odot$ pc^{-3} / 0.5 $\mathcal{M}_\odot$ as determined by the MACHO collaboration. A lower limit

of the absolute magnitude of the MACHOs is then given by $M_B = 21 - 5 \log r_2 + 5$, because MACHOs more distant than r_2 will not show up in the LHS, since they are fainter than the apparent magnitude limit of the LHS, $B = 21$ mag. From Table 3 we conclude that MACHOs are fainter than $M_B = 21.2$ mag. The southern hemisphere ($\delta < -30°$) and the galactic belt are not sampled by the LHS survey. Thus one could argue that only the region $b \geq 30°$ is properly sampled. This would reduce the numbers in the second column of Table 3 by a factor of 0.25 and shift the lower limit of the absolute magnitude of the MACHOs to $M_B = 20.6$ mag. If the distribution of MACHOs is irregular and lumpy, the micro-lensing results could mimic a too high mean density of MACHOs. If we assume a local MACHO density of only 10% of the value determined by the MACHO collaboration, the lower limit of the absolute magnitude of MACHOs would be $M_B = 20.1$ mag.

Table 3: Estimated absolute magnitudes of MACHOs.

r_N [pc]	N	M_B [mag]
6	0.31	22.1
9	2.3	21.2
12	9.4	20.6
15	27.3	20.1
18	64.0	19.7

If the MACHOs were identified with faint red dwarfs, their masses would be less than 0.1 $\mathcal{M}_\odot$ in contradiction to the estimate by the MACHO collaboration. As an alternative very faint white dwarfs have been discussed in the literature as MACHO candidates[23]. If we use the theoretically calculated cooling sequence of a DA white dwarf by Wood[24] and extrapolate $B-V$ to 2 mag, we estimate cooling times of 11 to 13 Gyrs for white dwarfs as faint as $M_B =$ 20.1 to 21.2 mag. This would make them as old as globular clusters and raises the question, whether this allows for reasonable lifetimes of the progenitors of the white dwarfs.

Acknowledgements

We are indebted to G. Gilmore for encouraging us to this research and C. Flynn, K. Freese, N.W. Evans, and R. Wielen for many valuable hints and comments.

We are grateful to J. Bahcall, C. Flynn, and A. Gould for making available to us the their data on the Groth strip prior to publication.

References

[1] C. Alcock et al., ApJ **461**, 84 (1996)
[2] R. Ansari et al., A&A **314**, 94 (1996)
[3] J.N. Bahcall, C. Flynn, A. Gould, and S. Kirhakos, ApJ **435**, L51 (1994)
[4] C. Flynn, A. Gould, and J.N. Bahcall, ApJ **466**, L55 (1996)
[5] D. Graff and K. Freese, ApJ **456**, L49 (1996)
[6] J. Liebert, in *Dark Matter*, AIP Conf. Proc. **336**, 71 (1995)
[7] H. Jahreiß and W. Gliese, in preparation (1996); preliminary version available on CD-ROM *Selected Astronomical Catalogs Vol. 1* eds. L.E. Brotzman and S.E. Gessner (ADC, NASA, Greenbelt 1991)
[8] S.K. Leggett, ApJS **82**, 351 (1992)
[9] M.T. Ruiz and C. Anguita, AJ **105**, 614 (1993)
[10] B.J. Taylor, PASP **106**, 704 (1994)
[11] I.N. Reid, S.L. Hawley, and J.E. Gizis, AJ **110**, 1838 (1995)
[12] H.R.A. Jones, A.J. Longmore, F. Allard, and P.H. Hauschildt, MNRAS **280**, 77 (1996)
[13] A.C. Layden, AJ **110**, 2288 (1995)
[14] D.R. Alexander et al., A&A, submitted (1996)
[15] R. Wielen, Mitt. Astron. Ges. **38**, 254 (1976)
[16] J.N. Bahcall, M. Schmidt, and R.M. Soneira, ApJ **265**, 730 (1983)
[17] C.C. Dahn, J. Liebert, H.C. Harris, and H.H. Guetter, in *The Bottom of the Main Sequence and Beyond*, ed. C.G. Tinney (Springer, Berlin), 239 (1995)
[18] C.J. Wetterer and J.T. McGraw, AJ **112**, 1046 (1983)
[19] G.W. Preston, S.A. Shectman, and T.C. Beers, ApJ **375**, 121 (1983)
[20] C.J. Pritchet and S. van den Bergh, AJ **107**, 1730 (1994)
[21] A. Gould, C. Flynn, and J.N. Bahcall, ApJ, submitted (1996)
[22] W.J. Luyten and A.E. La Bonte, *The South Galactic Pole*, (Univ. of Minnesota, Minneapolis 1973)
[23] S. Charlot and J. Silk, ApJ **445**, 124 (1995)
[24] M.A. Wood, in *White Dwarfs*, eds. D. Koester and K. Werner, (Springer, Berlin), 41 (1995)